JACS
JOURNAL OF THE AMERICAN CHEMICAL SOCIETY

Article

pubs.acs.org/JACS

A Mechanistic Hypothesis for the Aspirin-Induced Switch in Lipid Mediator Production by Cyclooxygenase-2

Paolo Tosco*

Department of Drug Science and Technology, Via Pietro Giuria 9, 10125 Torino, Italy

Supporting Information

ABSTRACT: Cyclooxygenase (COX) carries out stereospecific oxygen addition to arachidonic acid to generate prostaglandins, plus smaller amounts of 11- and 15-hydroxyeicosatetraenoic acids. For COX-2, the stereochemistry and relative abundance of generated products is influenced by Ser530 acetylation following aspirin treatment. The molecular bases of the high degree of stereospecificity which characterizes COX-2-catalyzed oxygenations are not yet completely understood, nor are the reasons behind the aspirin-induced shift in lipid mediator production. A mechanistic hypothesis is proposed which identifies steric shielding as the main determinant of oxygenation stereospecificity. This hypothesis is supported by a computational model which accurately reproduces experimental oxygenation patterns on both native and aspirin-inhibited COX-2.

INTRODUCTION

Prostaglandin endoperoxide H synthase (PGHS) is a bifunctional hemoprotein endowed with both cyclooxygenase and peroxidase activities; since the former constitutes the first committed step on the biosynthetic pathway leading from arachidonic acid (AA) to prostaglandins (PGs), this enzyme is often referred to as cyclooxygenase (COX).[1] Two isoforms of COX exist; while COX-1 is constitutive, the expression of COX-2 is induced during inflammatory states. Nonselective blockade of PG biosynthesis by traditional nonsteroidal anti-inflammatory drugs (NSAIDs) results in anti-inflammatory, analgesic and antipyretic effects, as well as undesirable gastrointestinal (GI) and renal toxicities. The active sites of the two isozymes share a high degree of structural homology (85%); however, the replacement of two isoleucine residues in COX-1 (Ile434 and, most importantly, Ile523) with valine makes the active site of COX-2 about 27% larger, thus enabling access to a side pocket which is almost obliterated in COX-1.[1,2] This side pocket, which compared to COX-1 features also the replacement of His513 with Arg513, was exploited to design a new class of COX-2-selective inhibitors, the coxibs. In principle, selective targeting of the inducible isoform should afford ideal NSAIDs, devoid of the ulcerogenic and nephrotoxic potential of traditional COX inhibitors. Unfortunately, clinical trials showed that a significantly higher number of adverse cardiovascular events were associated with selective COX-2 inhibitors compared to nonselective ones, while the benefit in terms of GI side effects was lower than expected. Cardiovascular events were attributed to the buildup of vasoconstrictor and pro-aggregatory thromboxane A_2 (TxA_2), generated by uninhibited COX-1. The outcome of these studies led to the withdrawal from the market of all coxibs except celecoxib.[2]

PGG_2 is the main product generated by COX upon dioxygenation of AA, with minor amounts of monooxygenated 11- and 15-hydroperoxyeicosatetraenoic (HPETE) acids. The heme-catalyzed peroxidase activity is required to reduce the hydroperoxy intermediates to their hydroxylated counterparts, namely, PGH_2 and hydroxyeicosatetraenoic acids (HETE), as well as to generate the Tyr385 radical which starts the catalytic cycle (Scheme 1).[3] Initially, the Tyr385 radical abstracts the 13-pro*S* hydrogen from AA (**1**), generating a delocalized C11−C15 pentadienyl radical (**2**) which undergoes antarafacial oxygen addition principally at C11, yielding 11*R*-HPETE (**3**); no 11*S* isomer is produced. A minor fraction of the pentadienyl radical adds O_2 at C15, yielding a mixture of 15*S* (**9s**) and 15*R*-HPETE (**9r**), the former being the most abundant epimer. As already mentioned, such HPETEs are reduced to the respective HETE (**4**, **10r**, **10s**) by peroxidase and constitute minor PGHS products.[4] Instead, the majority of **3** undergoes 9,11-cyclization yielding a C8-radical cyclic endoperoxide intermediate (**5**), followed by 8,12-cyclization yielding a C13−C15 allyl radical (**6**). The latter adds a second oxygen molecule at the 15-pro-*S* position to give PGG_2 (**7**), which is finally reduced by peroxidase to PGH_2 (**8**).

COX activity is substantially altered as a consequence of aspirin treatment. While acetylated COX-1 fails to generate any oxygenated products, in the case of COX-2 only PG generation is blocked, while the production of 11R- and 15-HETE is maintained.[5] Most interestingly, the *R*/*S* ratio between 15-

Received: March 21, 2013
Published: June 20, 2013

dx.doi.org/10.1021/ja402870k | J. Am. Chem. Soc. 2013, 135, 10404−10410

Scheme 1. AA Oxygenations Catalyzed by PGHS-2

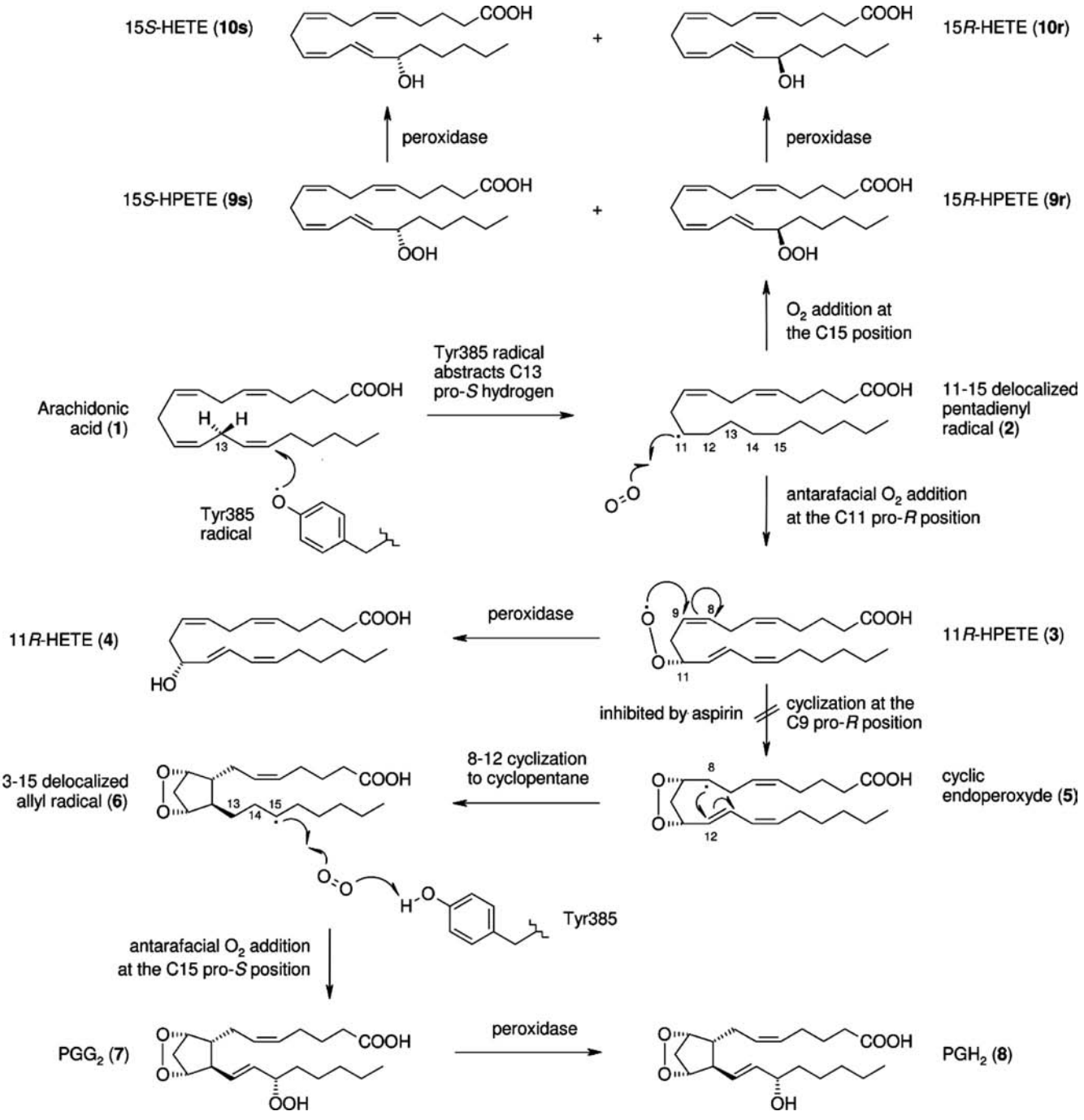

HETE epimers is reversed compared to the uninhibited enzyme.[6] This switch in lipid mediator production by COX-2 has important therapeutic implications: metabolites of 15*R*-HETE such as 15-*epi*-LXA_4 are endowed with potent pro-resolving activity, which sums up to the anti-inflammatory and antiaggregatory activity consequent to the blockade of PG/TxA_2 biosynthesis, making aspirin a unique, dual-acting irreversible COX inhibitor.[7]

Neither the mechanisms enforcing stereospecificity in AA oxygenation by native COX-2 nor the changes induced by aspirin treatment have been completely clarified so far.[3] In native COX-2, molecular dynamics (MD) simulations suggested that steric shielding and oxygen channeling determine the reactivity of the different carbon centers, which in turn influences the relative abundance and the stereochemistry of the products.[8] Regarding aspirin inhibited COX-2, Schneider and Brash hypothesized that the presence of an acetyl group on Ser530 forces a ω-tail twist of AA, which in turn would induce a reversal of C15 oxygenation stereochemistry, and at the same time would sterically shield C11 from reacting with oxygen.[9] This hypothesis however does not explain why 11*R*-HPETE is still produced by acetylated COX-2, and conflicts with later site-directed mutagenesis experiments,[5] which indicate that AA adopts an L-shaped binding mode very similar to the one recently elucidated by X-ray crystallography in uninhibited COX-2.[10]

Herein a computational model of COX-2-catalyzed lipid mediator production is presented, which led to the formulation

dx.doi.org/10.1021/ja402870k | J. Am. Chem. Soc. 2013, 135, 10404−10410

of a comprehensive hypothesis on the molecular mechanisms underlying oxygenation of AA in both the native and the aspirin-inhibited enzyme.

RESULTS AND DISCUSSION

According to previous quantum-mechanical/molecular-mechanical (QM/MM) studies of COX inhibition by aspirin,[11] the transfer of the acetyl group from acetylsalicylate to Ser530 proceeds under general base catalysis via a tetrahedral intermediate (Scheme 2): in the rate-determining step, the hydroxyl group of Ser530, following deprotonation by aspirin's carboxylate, carries out a nucleophilic attack on the acetyl carbonyl. Tyr385 has a twofold key role as a hydrogen bond donor in this mechanism, first in orienting and polarizing the carbonyl group, then in stabilizing the negatively charged tetrahedral intermediate.[11,12] The latter evolves to acetyl-Ser530 following elimination of salicylate, which diffuses out of the binding site.

Scheme 2. Proposed Mechanism for Ser530 Acetylation by Aspirin

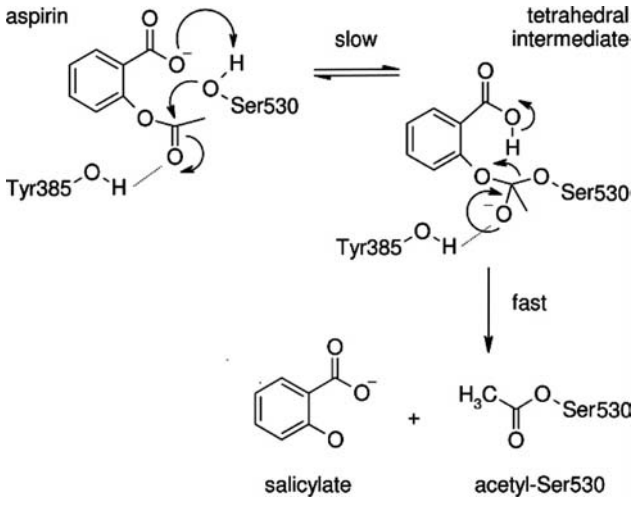

Based on those results, as well as on crystallographic evidence gathered on COX-1 by Loll and co-workers,[13] the acetyl-Ser530 side chain appears to hinder access to the COX top channel, the same where the productive conformation of **1** places its ω-end.[14] In contrast with this observation, it has been demonstrated by selected mutations (in particular V228F and G533A) that **1** adopts a similar conformation also in aspirin-inhibited COX-2.[5] Hence, alternative conformations for acetyl-Ser530 must exist which enable **1** to enter the top channel.

In the aforementioned QM/MM calculations a simulated annealing procedure was employed to identify Michaelis complexes suited for triggering the transacylation reaction between acetylsalicylate and Ser530; this procedure was intentionally biased toward productive poses by forcing the distance between the acyl carbon and Ser530 OH oxygen to be <3.5 Å. To avoid missing potential pro-acylating poses which do not preclude access to the top channel, in the present work a different, unbiased approach was followed. Namely, **1** was removed from the COX-2/**1** crystallographic complex (PDB ID 3HS5), then the tetrahedral intermediate resulting from the nucleophilic attack of deprotonated Ser530 on acetylsalicylic acid was built (Scheme 2),[11] and finally covalent docking of the acetyl-Ser530 adduct was carried out with AutoDock 4.2.[15] In all docking poses the acetyl moiety blocked the top channel, while the salicylate portion was located below the Tyr385-Ser530 constriction, the same region where competitive inhibitors bind (Figure 1A); therefore, this unbiased methodology confirmed the results previously obtained by simulated annealing.[11] After decomposing *in silico* the tetrahedral intermediate to salicylate and acetyl-Ser530, the latter assumed a pose very similar to the one adopted by bromoacetyl-Ser530 on COX-1[13] (heavy atom RMSD 1.17 Å, Figure 1B).

While this pose is consistent with crystallographic and theoretical studies, definitely it would not enable **1** to bind in a conformation similar to uninhibited COX-2.[4] This issue was tackled from a different perspective; namely, the same covalent docking methodology was followed, this time in the presence of **1**, in the same conformation experimentally found on native COX-2.[14] A unique binding pose was found where the acetyl group on Ser530 was accommodated beside **1**, whose binding mode was almost unchanged compared to the X-ray structure

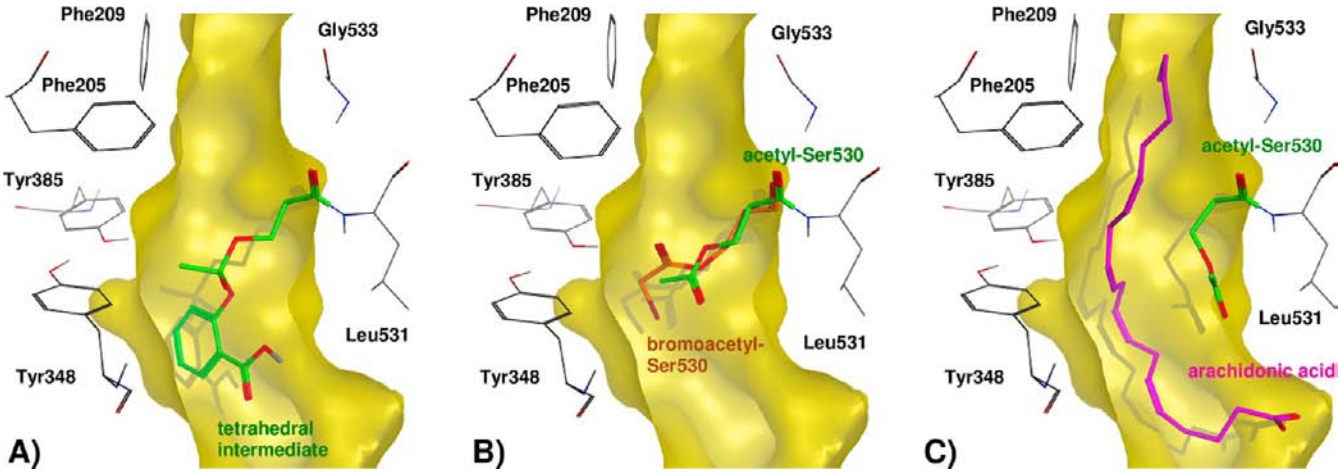

Figure 1. Docking poses within the COX-2 cavity (depicted via a Z-clipped yellow Connolly surface) of (A) the tetrahedral intermediate (green) originated by reaction between Ser530 and aspirin; (B) acetyl-Ser530 (green) following rupture of the tetrahedral intermediate; superimposed crystallographic coordinates of bromoacetyl-Ser530 are also included for comparison (orange); (C) acetyl-Ser530 (green) coexisting beside AA (magenta). 3D Rotatable WEOs are available for each image (see Movie 1, Movie 2, and Movie 3).

dx.doi.org/10.1021/ja402870k | J. Am. Chem. Soc. 2013, 135, 10404−10410

(heavy atom RMSD 0.84 Å, Figure 1C). Therefore, one could imagine a situation where: (a) Ser530 reacts with acetylsalicylate yielding a tetrahedral intermediate such as the one depicted in Figure 1A; (b) the tetrahedral intermediate evolves to acetyl-Ser530 in a conformation which still blocks the top channel (Figure 1B); (c) the side chain of acetyl-Ser530 moves below the Tyr385-Ser530 constriction (Figure 1C), thus allowing free access to **1**. To verify if acetyl-Ser530 may undergo such a rotameric shift, a 20-ns MD simulation of the acetylated enzyme in the absence of **1** was carried out, sampling 10,000 conformations along the trajectory. For each of them, the RMSD of acetyl-Ser530 heavy atoms from the docking pose depicted in Figure 1C was computed; more than 700 conformations of acetyl-Ser530 had a RMSD within 2.0 Å from the docking pose, the closest being 1.45 Å (see Movie 4). This means that the conformational flexibility of the acetyl-Ser530 adduct is actually large enough to allow binding of **1** in the top channel as in Figure 1C.

Subsequently, the complex between acetylated COX-2 and the pentadienyl radical **2** (obtained from **1** by abstraction of the pro-*S* hydrogen from C13) was subjected to MD; for comparison, the same simulation was performed also on the complex between **2** and uninhibited COX-2, in order to spot eventual differences in reactivity toward O_2 between native and acetylated enzyme. On both trajectories, 2500 conformations were sampled along the last 5 ns; selected average distances were measured and collected in Table 1. It can be observed that

Table 1. Selected Average Distances Collected along the MD Trajectories of Native and Aspirine-Inhibited COX-2

Distance[a]	Native COX-2	Acetylated COX-2
C13 - Tyr385(O)	3.26 Å	3.31 Å
C11 - Ser530	4.43 Å	4.44 Å
2 - Val523	4.75 Å	4.35 Å
C15 - {Ser530|Leu534}	4.23 Å	3.76 Å
C8 - C12	4.16 Å	4.55 Å

[a]When one or more residues/substrates are indicated, the shortest distance was considered from any of the constituting atoms.

there are no significant differences between the two complexes, as far as the portion of **2** inserted in the top channel is concerned. The average distance between C13 and Tyr385 hydroxyl oxygen is almost identical (~3.2 Å), indicating that the ease of 13-pro-*S* hydrogen abstraction is not affected by acetylation. The same consideration holds true for the average distance between C11 and the closest atom belonging to Ser530 (~4.4 Å). More significant differences arise in the portion of **2** lying below the Tyr385-Ser530 constriction: in acetylated COX-2, **2** gets about 0.4 Å closer to Val523, and C15 is on average 0.5 Å closer to either Ser530 or Leu534; conversely, C8 gets around 0.4 Å farther from C12 than in the native enzyme. Val523 has been proven to have a crucial role in the switch in lipid mediator biosynthesis by aspirin-inhibited COX-2: its mutation to Ile523 determines a 70% drop in 15-HETE production compared to the wild-type.[5] Since according to the simulation Val523 lies closer to **2** in the acetylated enzyme, it is not surprising that the increase in steric bulk moving from valine to isoleucine may determine a change in the conformation of **2** which affects its reactivity toward oxygenation to 15-HETE. Similarly, the fact that C15 lies closer to Ser530 and Leu534 (which face the 15-pro-*S* side of **2**) may hinder antarafacial pro-*S* addition of oxygen, thus reversing the *R*/*S* epimer ratio. Finally, the larger distance between C8 and C12 indicates that **2** adopts a more extended conformation, which may result in a lesser propensity to undergo cyclization into **7**.

To substantiate these hypotheses on quantitative grounds, a model was developed aimed at rationalizing the following three experimental observations: (1) O_2 reacts exclusively at the pro-*R* side of C11; (2) 9,11-cyclization does not occur on acetylated COX-2; (3) the *R*/*S* ratio of **9** epimers originated by oxygenation at C15 is reversed upon COX-2 acetylation. As already mentioned, MD simulations carried out by Furse et al.[8] support the involvement of steric shielding/oxygen channeling as the most important mechanisms (and possibly the only relevant ones[3]) enforcing the stereospecificity of oxygenation. No matter how it is channeled into the COX-2 cavity, to react at C11 and C15 O_2 needs to be located in their proximity, as well as to approach them with the correct geometry. Previous theoretical studies on the prereactant complexes between the pentadienyl radical derived from linoleic acid and molecular oxygen determined that the reactive carbon must not be too far from perpendicular with respect to the closest oxygen atom, at a distance between 3.0 and 4.0 Å.[16] Hence, two requirements were imposed for O_2 to be able to react at each carbon atom (Figure 2): (1) the C−O distance must not be greater than 3.5

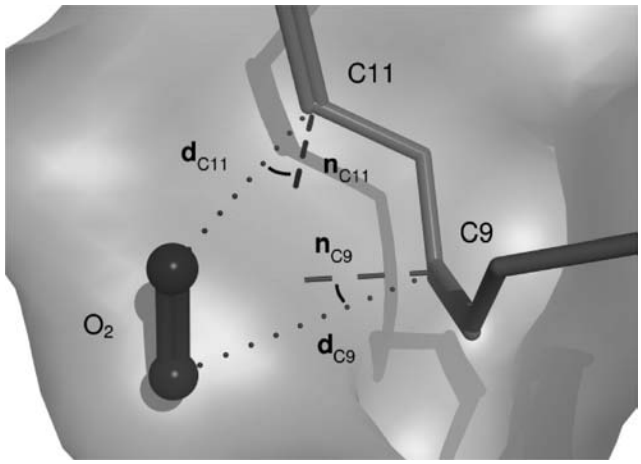

Figure 2. Geometric criteria used to evaluate the reactivity of the different O_2 docking poses toward addition at the carbon centers of **2**. The **d** vectors represent C−O distances, while **n** are normal vectors to the plane passing through C and the two neighboring carbons. A 3D rotatable WEO is available for this image (see Movie 5).

Å; (2) the angle between the C−O vector (**d**) and the vector passing through C, normal to the plane passing through C and the two neighboring carbons (**n**), must not be greater than 35°. With AutoDock Vina[17] O_2 was docked in vicinity of C11 and C15, respectively, using as docking targets the 2500 conformations extracted from the last 5 ns of the MD trajectory of the complexes between **2** and COX-2 (both native and acetylated). Finally, the number of poses for each target satisfying the aforementioned geometry requirements was counted. To quantify the propensity of **3** to undergo 9,11-cyclyzation yielding **4** (Scheme 1), it was imposed that distance and angle constraints be satisfied at the same time for C11 and for C9 (Figure 2). At first sight, this may appear as a crude approximation, since oxygen addition to C11 and C9 is not a concerted process. However, it has been demonstrated on COX-1 that if **2** does not have an appropriate conformation

(characterized by a specific K_m value) to yield **5** from the very moment O_2 reacts at C11, **3** will be generated instead, and the latter will not be converted to **7** anymore.[1,4] Therefore, it is reasonable to assume that also on COX-2 only conformations of **2** which from the beginning have the correct geometry to form a cyclic endoperoxide will yield **5**, while the others will not proceed beyond **3**. Results of the statistical analysis are collected in Table 2. For C11, all oxygen poses were pro-*R*,

Table 2. Comparison between Experimental and Calculated Percentages of HPETE Products Produced by Native and Acetylated COX-2

	Native COX-2		Acetylated COX-2	
product	exptl[a]	calcd	exptl[a]	calcd
11*S*-HPETE	0%	0%	0%	0%
11*R*-HPETE (**3**)	>99%	100%	<1%	0%
15*S*-HPETE (**9s**)	72%	73%	<1%	18%
15*R*-HPETE (**9r**)	28%	27%	>99%	82%

[a]Mouse COX-2 (ref 6).

in accordance with experimental evidence: in fact, no 11*S* products have ever been isolated.[3,8] On uninhibited COX-2, six poses were found potentially able to yield **3**, while two poses had an appropriate geometry to undergo cyclization to **5**. Instead, on acetylated COX-2 a single pose was found with the correct geometry to generate **3**, while none fulfilled the requirements to give **5**. Interestingly, loosening slightly the geometric criteria (4.0 Å distance, 40° angle) increases to 28 the poses yielding **5** on native COX-2, all quite similar to each other (average heavy atom RMSD 1.0 Å); in contrast, on the acetylated enzyme still no pose is able to trigger cyclization to **5**. Figure 3 puts into evidence the difference in the binding mode of **2** and the relative collocation of O_2 between native and acetylated COX-2. Looking at **2**, the main difference between the two structures lies in the value of the C9−C8−C7−C6 dihedral (native: −104°; acetylated: 94°), which results in the C5−C6 double bond lying on opposite sides with respect to the plane passing through C8,C7,C6. In other words, this means that **2** can get much closer to the Ser530 side of the channel in uninhibited COX-2, thus leaving a binding pocket for O_2 on the other side, delimited by Leu352 and Ser353. Conversely, in inhibited COX-2 the bulk of the acetyl group prevents **2** from approaching to Ser530. Instead, **2** is pushed against Leu352 and Ser353, thus obliterating the oxygen pocket on that side, while opening one beside Ser530; the latter has long been recognized as a putative oxygen pocket by crystallographic[18] and MD studies.[8] However, while from both pockets O_2 can react in an antarafacial fashion at C11 yielding the 11*R*-peroxide, only in the first case does the latter have the correct geometry to cyclize to **5**, while in the second case it is converted into **3** upon reduction by Tyr385. Moreover, as previously mentioned, the C8−C12 distance in the native enzyme is on average 0.4 Å lower, thus facilitating the subsequent attack of the radical at C8 on C12 to form a cyclopentane ring. Starting from the C11-pro-R pose of oxygen in native COX-2 depicted in Figure 3, the two sequential *in silico* cyclizations could be smoothly accomplished, obtaining first the COX-2 complex with **5**, then with **6** (Figures S2, S3; Supporting Information). Overall, this reactivity model provides a sound molecular basis for the blockade of prostanoid biosynthesis following COX-2 acetylation, amenable to small, but significant, differences in the conformation of **2**, which in

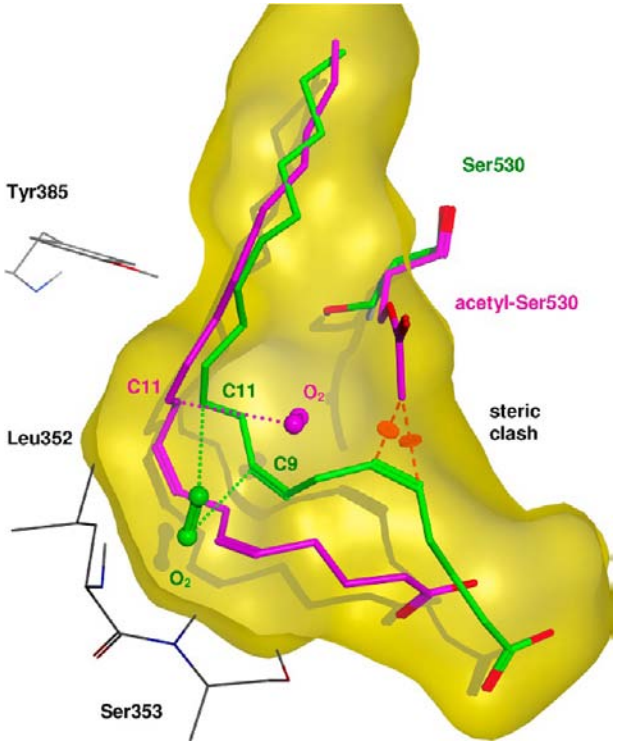

Figure 3. The two C11-pro-*R* conformations of **2** in native (green) and acetylated COX-2 (magenta), and the relative oxygen collocation. The steric clash that would take place between acetyl-Ser530 and **2** if the latter adopted the same conformation as in the uninhibited enzyme was evidenced with orange symbols. A 3D rotatable WEO is available for this image (see Movie 6).

turn influence the direction from which oxygen may react at C11.

Next, oxygenation at C15 of **2** yielding **9** was taken into consideration. **9** constitutes a minor product in native COX-2, with a sharp prevalence of the *S* isomer; instead, it becomes the main product following aspirin treatment, almost exclusively as the *R* isomer. As for C11, O_2 was docked in vicinity of C15 on all conformations extracted from the last 5 ns of the MD trajectories, filtering the obtained poses with the same geometric criteria used for the reaction at C11 (Figure 2). Two distinct clusters of poses were found, namely, pro-*S* and pro-*R* (Figure 4); quantitative data are collected in Table 2, together with the percentages of the two epimers of **9** experimentally assessed for murine COX-2.[6] There is a remarkable accordance between theoretical and experimental figures, the number of pro-*S* poses on acetylated COX-2 being slightly overestimated. Loosening or tightening the geometric criteria does not make a dramatic difference: the inversion of the *R*/*S* ratio upon aspirin treatment is still correctly captured by the model. In pro-*S* poses oxygen is located near Ser530, on the opposite side of **2** with respect to Tyr385, as expected for an antarafacial addition mechanism. Instead, in pro-*R* poses oxygen is located in a pocket delimited by Phe205, Phe209, and Tyr385, just above the latter; from that position, addition of O_2 at C15 would take place in a suprafacial fashion. This hypothesis has been previously formulated by Lecomte and co-workers, who published one of the earliest reports describing the switch in lipid mediator production by COX-2 upon acetylation,[19] and was later supported also by Thuresson et al.;[4] indeed, some fungal lipooxygenases are known to catalyze

dx.doi.org/10.1021/ja402870k | J. Am. Chem. Soc. 2013, 135, 10404−10410

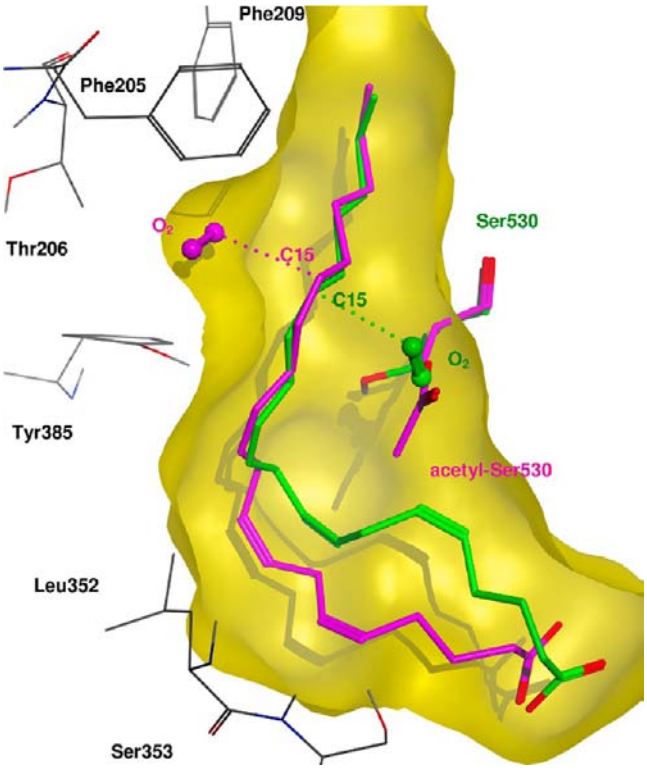

Figure 4. The C15-pro-*S* (green) and C15-pro-*R* (magenta) conformations of **2** in native and acetylated COX-2, respectively. A 3D rotatable WEO is available for this image (see Movie 7).

suprafacial O_2 addition.[20] While in principle there are no reasons to reject such a hypothesis,[3,9] the lack of experimental proof on human isoforms has prompted an alternative explanation for **9r** formation in acetylated COX-2: the steric bulk due to the acetyl group would induce a ω-tail twist on **2**, thus modifying the stereochemistry at C15 while maintaining the antarafacial mechanism of O_2 addition.[9] However, as anticipated in the Introduction, this possibility conflicts with mutational data gathered by Rowlinson et al.,[5] which indicate that the ω-tail of **2** adopts a similar binding mode in both native and aspirin-inhibited COX-2. Even more importantly, if the formation of **9r** in aspirin-inhibited COX-2 were amenable to a conformational change of **2** induced by the bulky acetyl group on Ser530, then the significant amount of **9r** generated by native COX-2 could hardly be explained.[6] Therefore, based on computational and experimental evidence, suprafacial addition appears as the most convincing mechanism for pro-*R* oxygenation at C15, both in native and aspirin-inhibited COX-2.

CONCLUSIONS

A computational hypothesis for the molecular mechanisms governing AA oxygenation by COX-2 was presented, aimed at explaining their alteration upon enzyme acetylation by aspirin. According to this hypothesis, stereospecificity depends on the capacity of oxygen to approach the reactive carbons of AA with the correct geometry, which in turn is influenced by the degree of steric shielding exerted by the enzyme environment. The acetyl group transferred by aspirin to Ser530 has a twofold impact on oxygen reactivity toward AA. On one side, it alters the AA conformation enough to prevent the generation of the cyclic endoperoxide; on the other, it increases the shielding of the AA side opposite to Tyr385, to the extent that the direction of O_2 addition at C15 shifts from antarafacial to suprafacial. The quantitative model based on these assumptions can accurately predict the relative amounts of oxygenated lipid mediators on both native and aspirin-inhibited COX-2, thus providing a robust validation of the underlying mechanistic hypothesis.

Future work will focus on the identification of suitable channeling routes conveying oxygen to the relevant cavities in the enzyme. This theoretical study will hopefully awaken interest in the long-standing puzzle of the stereochemistry of AA metabolites generated by COX, prompting experimental investigations which may support (or eventually contradict) the mechanistic hypothesis presented here.

ASSOCIATED CONTENT

Supporting Information

Computational methods, AMBER parameter files for non-standard residues, Figures S1−S3. This material is available free of charge via the Internet at http://pubs.acs.org.

AUTHOR INFORMATION

Corresponding Author

paolo.tosco@unito.it

Notes

The authors declare no competing financial interest.

ACKNOWLEDGMENTS

This work was supported by the Chemical Computing Group (Montreal, Quebec, Canada) and COSMO*logic* (Leverkusen, Germany). I thank Prof. Alberto Gasco for helpful discussions.

REFERENCES

(1) (a) Smith, W. L.; DeWitt, D. L.; Garavito, R. M. *Annu. Rev. Biochem.* **2000**, *69*, 145−182. (b) Fitzpatrick, F. A. *Curr. Pharm. Des.* **2004**, *10*, 577−588.
(2) Marnett, L. J. *Annu. Rev. Pharmacol. Toxicol.* **2009**, *49*, 265−290.
(3) Schneider, C.; Pratt, D. A.; Porter, N. A.; Brash, A. R. *Chem. Biol.* **2007**, *14*, 473−488.
(4) Thuresson, E. D.; Lakkides, K. M.; Smith, W. L. *J. Biol. Chem.* **2000**, *275*, 8501−8507.
(5) Rowlinson, S. W.; Crews, B. C.; Goodwin, D. C.; Schneider, C.; Gierse, J. K.; Marnett, L. J. *J. Biol. Chem.* **2000**, *275*, 6586−6591.
(6) Schneider, C.; Boeglin, W. E.; Prusakiewicz, J. J.; Rowlinson, S. W.; Marnett, L. J.; Samel, N.; Brash, A. R. *J. Biol. Chem.* **2002**, *277*, 478−485.
(7) (a) Serhan, C. N. *Prostaglandins Leukot. Essent. Fatty Acids* **2005**, *73*, 141−162. (b) Serhan, C. N.; Chiang, N.; Van Dyke, T. E. *Nat. Rev. Immunol.* **2008**, *8*, 349−361.
(8) Furse, K. E.; Pratt, D. A.; Schneider, C.; Brash, A. R.; Porter, N. A.; Lybrand, T. P. *Biochemistry* **2006**, *45*, 3206−3218.
(9) Schneider, C.; Brash, A. R. *J. Biol. Chem.* **2000**, *275*, 4743−4746.
(10) Vecchio, A. J.; Simmons, D. M.; Malkowski, M. G. *J. Biol. Chem.* **2010**, *285*, 22152−22163.
(11) Tosco, P.; Lazzarato, L. *ChemMedChem* **2009**, *4*, 939−945.
(12) Hochgesang, G. P., Jr.; Rowlinson, S. W.; Marnett, L. J. *J. Am. Chem. Soc.* **2000**, *122*, 6514−6515.
(13) Loll, P. J.; Picot, D.; Garavito, R. M. *Nat. Struct. Biol.* **1995**, *2*, 637−643.
(14) Vecchio, A. J.; Simmons, D. M.; Malkowski, M. G. *J. Biol. Chem.* **2010**, *285*, 22152−22163.
(15) Morris, G. M.; Huey, R.; Lindstrom, W.; Sanner, M. F.; Belew, R. K.; Goodsell, D. S.; Olson, A. J. *J. Comput. Chem.* **2009**, *16*, 2785−2791.
(16) (a) Suardíaz, R.; Masgrau, L.; Lluch, J. M.; González-Lafont, À. *J. Phys. Chem. B* **2013**, *117*, 3747−3754. (b) Tejero, I.; González-

Lafont, À.; Lluch, J. M.; Eriksson, L. A. *J. Phys. Chem. B* **2007**, *111*, 5684−5693.
(17) Trott, O.; Olson, A. J. *J. Comput. Chem.* **2010**, *31*, 455−461.
(18) Malkowski, M. G.; Ginell, S. L.; Smith, W. L.; Garavito, R. M. *Science* **2000**, *289*, 1933−1937.
(19) Lecomte, M.; Laneuville, O.; JiS, C.; DeWitt, D. L.; Smiths, W. L. *J. Biol. Chem.* **1994**, *269*, 13207−13215.
(20) Hamberg, M.; Su, C.; Oliw, E. *J. Biol. Chem.* **1998**, *273*, 13080−13088.